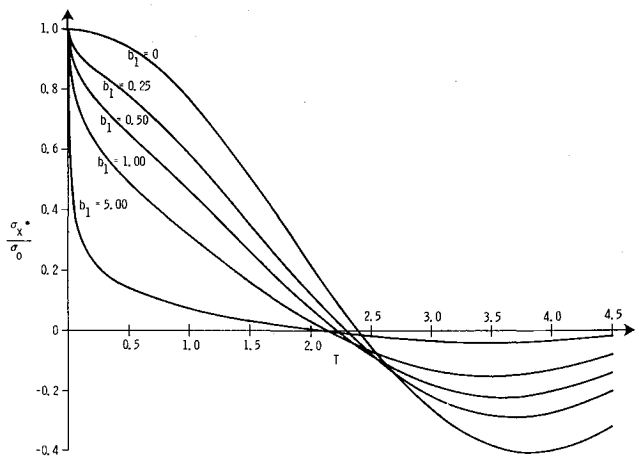

Fig. 3 Bending stress at the radially outward shell surface for $X = 0$.

Equation (6) is evaluated by considering the contour and branch cuts shown in Fig. 2. Utilizing Cauchy's theorem, the formal integral solution is replaced by the contributions of the poles of the integrand within the contour and the line integrals along l_1, l_2, and l_3. In general, the integrand has a pole at each of the two points where $F(s) = b_o + b_1(1 + s^2)^{3/4} + s^2 = 0$. For $b_0 < 1$, a detailed analysis of $F(s)$ indicates that two complex conjugate poles are located on the imaginary axis within $|Im(s)| < 1$. When $b_o > 1$, the theorem of the argument[3] can be used to show that the two poles are located in the s plane where $Re(s) < 0$ and $|Im(s)| > 1$, simultaneously.

However, for the interesting case where the ring and shell are of the same material $b_o = a_o = 1$, and the transformed solution reduces to

$$\bar{\sigma}_x^*/\sigma_o = 1/(1 + s^2)^{1/4}[b_1 + (1 + s^2)^{1/4}] \quad (7a)$$

$$\sigma_o = 3^{1/2}cI/(1 - \nu^2)^{1/2}h(1 + 1/n);\ b_1 = 2^{3/2}/\alpha^{1/2}L(1 + n) \quad (7b)$$

The integrand given by Eq. (7a) has no poles and the bending stress σ_x^* at the outer shell surface for $X = 0$ is given by

$$\frac{\sigma_x^*}{\sigma_0} = -\frac{1}{\pi}\int_0^\infty \times \frac{e^{-uT}[(b_1 + \rho\cos\alpha)\sin(T - \alpha) - \rho\sin\alpha\cos(T - \alpha)]}{\rho(b_1^2 + 2b_1\rho\cos\alpha + \rho^2)}\,du + \frac{1}{\pi}\int_0^1 \frac{\cos uT}{(1 - u^2)^{1/4}[b_1 + (1 - u^2)^{1/4}]}\,du \quad (8a)$$

$$\rho = u^{1/4}(4 + u^2)^{1/8};\ \alpha = 3\pi/8 + \psi/4;\ \psi = \cos^{-1}[2/(4 + u^2)^{1/2}] \quad (8b)$$

In Eq. (8a), the first integral is the contribution along l_1 and l_3 and the second integral is the contribution along l_2. The integrals in Eq. (8a) can be made proper by the substitution $u = v^2$ in the first integral and $u = 1 - v^2$ in the second integral.

Numerical Results

Equation (8a) was evaluated numerically for several values of the parameter b_1. Figure 3 shows the bending stress history in the outer shell fibers at the ring support for the case where the ring and shell materials are the same and $b_1 = 0, 0.25, 0.50, 1.00$, and 5.00. The bending stresses asymptotically approach zero for large values of time. Decreasing values of b_1 correspond to the ring becoming more massive relative to the shell. From Ref. 1, for a clamped boundary condition at $X = 0$, the bending stress at $T = 0$ is $\sigma_x^* = 3^{1/2}cI/[(1 - \nu^2)h]$; therefore, for an elastic ring, the bending stress at $X = T = 0$ is reduced by the factor $1/(1 + h/h_r)$.

References

[1] Sagartz, M. J. and Forrestal, M. J., "Transient Stresses at a Clamped Support of a Circular Cylindrical Shell," *Journal of Applied Mechanics*, Vol. 36, No. 2, June 1969, pp. 367-369.

[2] Baron, M. L., "Circular-Symmetric Vibrations of Infinitely Long Cylindrical Shells with Equidistant Stiffeners," *Journal of Applied Mechanics*, Vol. 23, No. 2, June 1956, pp. 316-318.

[3] Kaplan, W., *Operational Methods for Linear Systems*, Addison-Wesley, Reading, Mass., 1962, pp. 156-158.

Vortex Shedding from Circular Cylinders in an Oscillating Freestream

C. F. Chen* and David B. Ballengee†
Rutgers University, New Brunswick, N. J.

I. Introduction

Vortex shedding (i.e., from smoke stacks, missiles erected on the launch pad, and tall buildings) due to atmospheric wind is a complicated phenomenon because a) the flow is sheared in the atmospheric boundary layer, b) the flow is generally unsteady, and c) there are three-dimensional effects due to finite height. The effect of flow shear on vortex shedding from circular cylinders has been investigated by Chen and Mangione[1] for a Reynolds number range of 200 to 800. The results show that the local Strouhal and Reynolds numbers, in which characteristic velocity is that of the local approaching stream, correlate in much the same manner as those found for uniform flow. Recently we have concluded a series of experiments on vortex shedding from circular cylinders in an oscillating free stream. The Reynolds number range tested was from 500 to 4×10^4, and the frequencies of oscillation were 3 and 6 Hz. The experimental procedure and results are summarized below.

II. Experimental Apparatus and Procedure

A sketch of the wind tunnel used is shown in Fig. 1. The prime mover is an air-to-air ejector using high-pressure air at 125 psig. A muffler box is placed around the secondary air inlet and it is lined with acoustical insulation to reduce the noise level. Oscillation of the freestream is obtained by a butterfly valve placed downstream of the primary air nozzle.

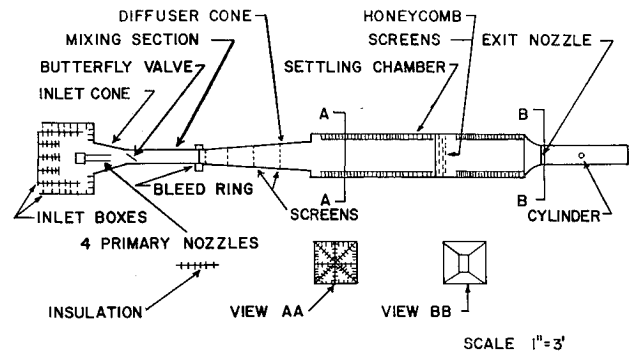

Fig. 1 Sketch of the oscillating flow wind tunnel.

Received September 16, 1970; revision received October 19, 1970. Research sponsored by AFOSR, Office of Aerospace Research, United States Air Force, under Contract F 44620-68-C-0018, monitored by D. L. Calvert.

* Professor of Aerospace Engineering. Member AIAA.

† Research Assistant, Department of Mechanical & Aerospace Engineering; now at Jersey Central Power and Light Company, Parsippany, N. J.

The butterfly valve is driven by a Zero-Max variable speed motor through a four-bar linkage with one variable length member. It is capable of producing an oscillating stream with frequency up to 6 Hz and with half-amplitude up to 50% of the mean flow velocity. The walls of the settling chamber are also lined with acoustical insulation for noise reduction purposes. A set of honeycombs and six 18-mesh screens are installed to reduce the turbulence level of the flow. The test section is 5 in. × 10 in. high, and it exhausts into the atmosphere. More detailed description of the wind tunnel can be found in Caldwell.[2]

Cylinders of 0.043 in., 0.2495 in. and 1.125 in. diam were tested. There were mounted externally to the test section to avoid any extraneous vibration transmitted from the test section walls. The two smaller size cylinders were installed under tension to raise the natural frequencies of vibrations beyond the range encountered due to vortex shedding.[3] Two hot wire probes were used to obtain the data; one is mounted on one side of the wake region to monitor the vortex shedding and the other is in the freestream. Both probes were mounted at the same vertical plane so that they are in phase. The signal from the probe measuring the freestream velocity was linearized and fed into one channel of a dual beam oscilloscope such that the velocity was represented as the height of the trace above a zero line. The output from the second probe was filtered to remove the freestream variations and then applied to the second channel of the oscilloscope. The traces were photographically recorded, from which the data were obtained.

III. Results and Discussion

A typical record from an X-Y plotter showing the oscillation of the freestream is presented in Fig. 2. The X coordinate is the time and the Y coordinate is the linearized voltage output of the freestream hot wire probe. The maximum and minimum velocities are 61.5 and 23 fps, respectively, and the frequency of oscillation is 3 Hz. The half-amplitude is 45.5% of the mean velocity. The oscillations are not quite sinusoidal; the ratio of the time required for the upswing to that for the downswing is approximately 4:3.

Three typical traces of the Dual-Beam Oscilloscope are shown in Fig. 3. For each record, the frequency ω, the diameter of the cylinder d, the mean Reynolds number Re_m ($=Umd/\nu$, where U_m is the mean velocity of the freestream and ν the kinematic viscosity), and the sweep rates S_ω for the vortex shedding probe and S_f for the freestream probe are given for each case. Figure 3a shows a 0.043-in. diam cylinder in a 3 Hz oscillating flow with $\mathrm{Re}_m = 780$. The lower trace is that of the freestream; the zero line is indicated by the pointer. Because of the relatively high sweep rate 2×10^{-3} sec/div, the freestream variation is hardly noticeable. The shedding frequency as indicated by the upper trace is almost constant during the entire time interval, and the shedding is very regular in appearance. Figure 3b shows a 0.2495-in. diam cylinder in a 6 Hz oscillating flow with $\mathrm{Re}_m = 6960$. The sweep rate is 5×10^{-3} sec/div. As the freestream velocity decreases, the shedding frequency decreases correspondingly. The shedding appears to be very regular.

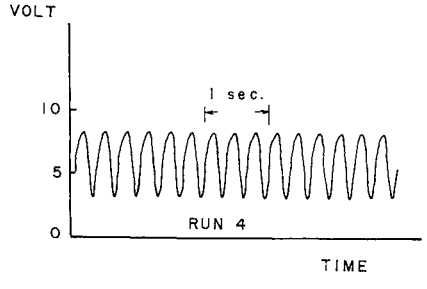

Fig. 2 Typical records of freestream velocity.

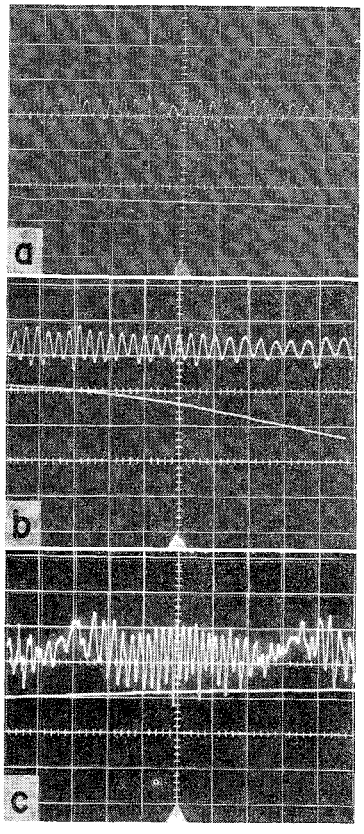

Fig. 3 Dual-beam oscilloscope traces. a) $\omega = 3$ Hz, $d = 0.043$ in., $\mathrm{Re}_m = 780$, $S\omega = S_f = 2 \times 10^{-3}$ sec/div. b) $\omega = 6$ Hz, $d = 0.2495$ in., $\mathrm{Re}_m = 6960$, $S\omega = S_f = 5 \times 10^{-3}$ sec/div., c) $\omega = 3$ Hz, $d = 1.125$ in., $\mathrm{Re}_m = 20{,}000$, $S_\omega = 5 \times 10^{-2}$ sec/div., $S_f = 5 \times 10^{-3}$ sec/div.

Fig. 3c shows the 1.125-in. diam cylinder in a 3 Hz oscillating flow with $\mathrm{Re}_m = 20{,}000$. For this case S_ω is ten times slower than $S_f = 5 \times 10^{-3}$ sec/div. Only one datum point can be obtained from this photograph. The trace of the vortex shedding probe exhibits $1\frac{1}{2}$ cycles in this picture. In the vicinity of the minimum velocity, the shedding frequencies become smaller and the shedding becomes quite irregular.

A total of 11 test runs were made, nine of which were 3 Hz and two of which were at 6 Hz for the 0.2495-in. cylinder. The ratio of the half-amplitude to the mean velocity varied from 29% to 45.5%. A total of 33 useful photographs were taken from which 42 data points were obtained. These data points are correlated as shown in Fig. 4 using the instantaneous Strouhal number ($=fd/U$) and the instantaneous Reynolds number ($= Ud/\nu$), where f is the shedding frequency and U the instantaneous freestream velocity. Superimposed on the point is the correlation recommended by

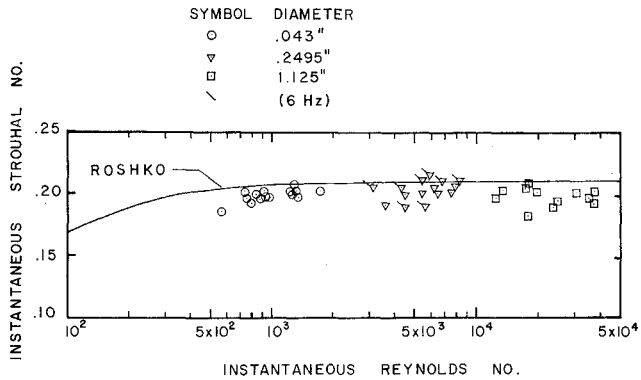

Fig. 4 Correlation of instantaneous Strouhal number with instantaneous Reynolds number.

Roshko[4] for vortex shedding in steady flow. Our data points in general are lower than the Roshko curve, however, they do show a definite correlation between the instantaneous Strouhal and Reynolds numbers. These results suggest the following conclusions: 1) In an oscillatory freestream of 3 Hz and Reynolds number up to 4×10^4, the vortex shedding from a circular cylinder responds instantaneously to the freestream variations. 2) In the instantaneous Reynolds number range of 500 to 4×10^4, the instantaneous Strouhal number stays sensibly constant at 0.20, ± 0.01. 3) With a limited set of data points in the instantaneous Reynolds number range of 3 to 8×10^3, the results show no systematic variation when the frequency is increased from 3 to 6 Hz.

References

[1] Chen, C. F. and Mangione, B. J., "Vortex Shedding from Circular Cylinders in Sheared Flow," *AIAA Journal*, Vol. 7, No. 6, June 1970, pp. 1211–1212.

[2] Caldwell, J. B., "Experimental Investigation of Laminar Skin Friction under Oscillating Flow," Ph.D. thesis, Jan. 1970, Department of Mechanical and Aerospace Engineering, Rutgers University, New Brunswick, N. J.

[3] Van Atta, C. W., "Experiments on Vortex Shedding from Yawed Circular Cylinders," *AIAA Journal*, Vol. 6, No. 5, May 1968, pp. 931–933.

[4] Roshko, A., "Experiments on the Flow Past a Circular Cylinder at Very High Reynolds Number," *Journal of Fluid Mechanics*, Vol. 10, 1961, p. 345.

Comparison of Theory and Experiment for Ion Collection by Spherical and Cylindrical Probes in a Collisional Plasma

JOHN A. THORNTON*

Telic Corporation, Santa Monica, Calif.

THIS Note describes double probe ion saturation current measurements made with spherical and cylindrical probes in a helium negative glow plasma operated in the transitional pressure range for the probe sizes tested. The results are compared with two currently available transitional regime probe theories. In addition a relatively simple formulation is described which approximates the more rigorous theories.

If a formal sheath boundary is postulated, the current I_p to a negatively biased probe in a plasma that contains a single positive ion species can be expressed in terms of the sheath ion flux; i.e.,

$$I_p = e\phi A_s n_s u_s = e\phi A_p n_0 u_s (A_s/A_p)(n_s/n_0) \qquad (1)$$

where n is the density and u the velocity of the ions, A the surface area, e the electronic charge, and ϕ the fraction of ions crossing the sheath that reach the probe. The subscripts s and p refer to the sheath and probe surfaces. Since ion current measurements are generally used to estimate the plasma electron (ion) density n_0, suitable theories must relate $u_s\phi(A_s/A_p)(n_s/n_0)$ to parameters, such as the electron and ion temperatures (T_e and T_i) and the gas density, which can be determined by other techniques.

Laframboise[1] treated the collisionless case for spherical and cylindrical probes. His results—presented as a tabulation of a parameter i such that

$$I_p = eA_p n_0 (kT_e/2\pi M_i)^{1/2} i(V_p/kT_e,\ r_p/\lambda_d,\ T_i/T_e) \qquad (2)$$

where V_p is the probe potential (relative to the plasma), r_p the probe radius, and λ_d the Debye length—have been verified experimentally, for the cylindrical case, by comparison with microwave measurements.[2] Kiel[3] has reviewed the collision dominated case ($\lambda_i \ll \lambda_d$, where λ_i is ion mean free path) and derived approximated relations which can be written as

$$(I_p)_{\text{sphere}} = eA_p n_0 (A_s/A_p)_c\, \mu_i k(T_e + T_i)/r_s \qquad (3)$$

$$(I_p)_{\text{cyl}} = eA_p n_0 (A_s/A_p)_c\, [\mu_i k(T_e + T_i)/r_s]\ 1/\ln(\pi L/4r_s) \qquad (4)$$

where μ_i is the ion mobility, L is the length of a cylindrical probe, and semiempirical expressions are given for r_s/r_p. Several attempts have been made to develop a sufficiently general theory to handle the transition regime between the collisionless and collision dominated cases.[4–7] The theory of Chou et al.,[4] although difficult to use, is believed to be the most rigorous. From this theory Talbot and Chou[5] have constructed manageable approximations for both spherical and cylindrical probes. Self and Shih[6] have presented useful data for spherical probes. Although the Talbot-Chou and Self-Shih theories are in general agreement, yielding the Laframboise results in the collisionless limit, and essentially the result approximated by Kiel in the collision dominated limit, the Talbot-Chou theory predicts slightly lower currents in the transitional range (see Figs. 1 and 2). Waymouth[7] formulated a theory for the spherical probe thin sheath case by solving the diffusion equations in the quasi-neutral region and matching the solution to the collisionless thermal flux at the sheath edge. His results do not agree with Laframboise's in the collisionless limit because of a failure to include ion inertia effects in the diffusion equations.

An examination of the published numerical results for the collisionless and collision dominated cases permits the following observations for negatively biased probes of practical size for laboratory plasmas ($r_p/\lambda_d > 10$, $\phi = 1$). 1) The probe current is controlled primarily by the electric field in the quasi-neutral region. In the collisionless case this field causes a moderate density decrease ($n_s/n_0 \sim 0.5$) and a significant ion acceleration [$u_s \sim (kT_e/M_i)^{1/2}$]. In the collision dominated case the quasi-neutral field extends farther into the plasma, the density decrease is large ($n_s/n_0 \sim 0.1$), and the ion acceleration should remain significant.[8,9] 2) The primary significance of the sheath edge per se is in determining the effective capture area of the probe. These observations suggest that a relatively simple transition regime probe theory can be formulated by matching a collision dominated quasi-neutral region with a collisionless inertia controlled formulation such as that of Laframboise.[1] This approach is possible because as collisions become important their first-order effect is to increase the density drop in the quasi-neutral region, thereby effectively establishing new boundary conditions for the collisionless sheath. When the density is so high that collisions become important in the sheath, the ion transport is dominated by the large density drop in the quasi-neutral region, and the model's assumption of a collisionless sheath does not introduce a large error. A similar situation holds for u_s. In the collision dominated limit u_s cancels out of the formulation. As one passes into the transition regime inertia effects become increasingly important in the quasi-neutral region, and the assumption that u_s is approximately equal to $(kT_e/2\pi M_i)^{1/2}$ (the value implied by the collisionless theory) appears realistic.[8,9]

Consider the case of a spherical probe. The collision induced density drop across the quasi-neutral region of a negatively biased probe with a collisionless sheath can be written as[7]

$$n_s/n_0 = 1/[1 + u_s r_s/\mu_i k(T_e + T_i)] \qquad (5)$$

Received September 9, 1970.

* Director of Research and Development. Associate Fellow AIAA.